Terrain Jumper: Locust Robot Design and Application Combined with Mathematical Modeling

Xinyi Shi, Ziyuan Xu

Nanjing Foreign Language School, Nanjing 210008, China

Abstract

This study is based on bionics. The jumping model of a locust-based robot was designed and manufactured through analysis and study of the jumping behavior of locusts. Experiments verified that the locust robot model has good jumping ability and stability, further expanding special application scenarios such as robots moving in rough terrain.This study uses a one-sided locust model and a six-link model as a simulation structure based on existing literature research. According to the position state of the Robot during the jump, a mathematical model is established to analyze the jump. Continuous structural adjustments finally created a locust bionic robot with strong jumping ability. The experiment revealed that the Robot will roll over and fall due to an unstable center of gravity during jumping. This study further designed an auxiliary automatic correction structure mainly controlled by a steering gear.

Keywords

Locust robot, bionics, dynamic model, jumping model, mechanism design.

1. Introduction

1.1. Research Background and Significance

Bionics involves the study of natural biological systems, focusing on extracting design principles from their structural and functional elements for use in modern robotic engineering. Terrestrial robots are typically divided into four categories: wheels, serpentine designs, legged motion, and jumping mechanisms. Although wheeled and serpentine robots are well-advanced, their smaller counterparts face substantial difficulties when maneuvering over obstacles and traversing uneven terrain. For example, while small wheeled robots can move swiftly on flat surfaces, they often find it challenging to pass over barriers that exceed twice the diameter of their wheels.

2. Analysis of the Locust Robot Jumping Model

2.1. Establishment of a Jumping Mechanism Model

Locusts utilize the contractile forces generated by the extensor tibial muscles in their hind legs to power their jumps. In jumping, the back leg quickly completes the change from folding to stretching, instantly releasing the energy generated by muscle contraction and completing the jumping process. Due to the symmetry of the locust's body, in order to facilitate subsequent modeling, we can only consider the one-sided model.

By studying the locust's rear leg structure and jumping method, we established a six-link simulation structure and used springs as a power storage device.When the spring energy is released, it simulates the locust's jumping process, first stretching the tibia (EH in the picture) and then instantaneously converting this energy into the ground's reaction force against the tarsal bone through a connecting rod to complete the jump.

2.2. Jumping Process Modeling

Generally speaking, the jumping process of a jumping robot can be divided into three stages: the takeoff stage, the airborne stage, and the landing stage.

2.2.1. Jumping Phase

According to the position of the shin bone in its initial state, the takeoff process is divided into the following two stages.

2.2.2. Airborne Phase

When the Robot leaves the ground and enters the airborne phase, the overall motion trajectory and equation can be equivalent to a mechanical flat throw model without considering ideal conditions such as air friction. In other words, vertical kinetic energy is converted into gravitational potential energy, moving at a uniform speed in the horizontal direction, and the vertical velocity is 0 when reaching the highest point.

2.2.3. Landing Stage

Since the jumping process in this article only considers that the Robot is affected by gravity, other external influences, such as air resistance, are ignored. Therefore, during the landing phase, the Robot's kinetic energy is consistent with the takeoff time, and other influencing factors will be considered in the subsequent research process, thereby improving the stability of the overall movement.

2.3. Analysis of the Jumping Ability of Jumping Robots

The criteria for evaluating a robot's jumping ability can be divided into two types: one is the overturning problem, where the Robot's jumping trajectory can cover an obstacle to determine whether it can jump smoothly; the other is the climbing problem, where the Robot's motion target is above the object. This usually happens when a single jump cannot completely cross the obstacle but can reach the expected height through multiple climbs to achieve the ultimate goal.

2.3.1. The Effect of Takeoff Distance on Jumping Ability

In response to the rollover problem, considering that the size of the jumping robot's shape affects overturning the obstacle, we increased the Robot's external size to the size of the obstacle, thereby ignoring the shape and simplifying the motion process to particle motion for analysis.

2.3.2. The Effect of the Initial Takeoff Angle on Jumping Ability

Through analysis of the movement trajectory, it can be found that due to differences in sum, there will also be differences in jumping curves, and there will also be big differences in jumping ability. Therefore, when the position and shape of the obstacle are known, we can obtain the optimal motion trajectory for a specific obstacle by controlling the initial angle of the Robot's long jump.

3. Theoretical Design

The theoretical design is the first version of the locust bionic robot. Starting with this section, there are four versions of robots. The main purpose is to verify the mathematical model's formula further and achieve the best possible height and distance.

In the design process, preliminary robot structural design and functional module division are carried out according to the locusts' jumping characteristics and the Robot's application requirements. Using hand-drawn sketches and 3D modeling software, it can be designed to form a preliminary robot design plan.

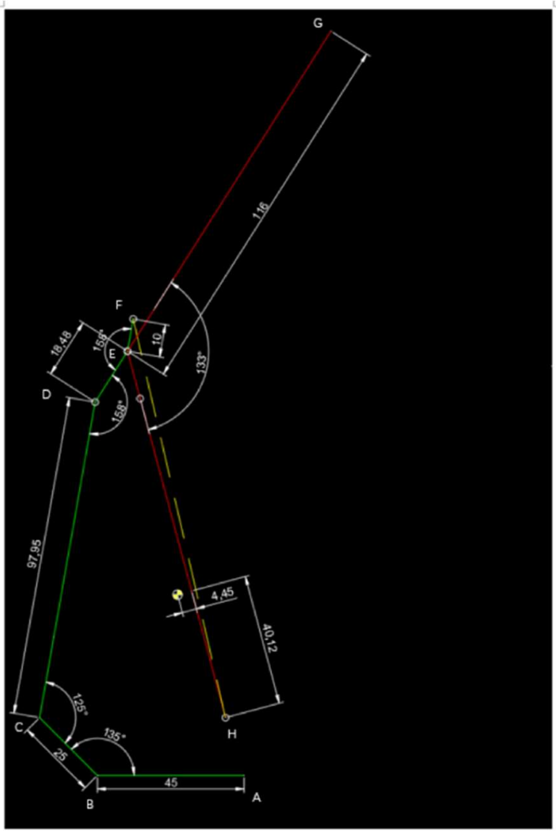

Figure 1. Schematic diagram of the structure

4. Structure Design

4.1. First Edition

In the overall structural design, the bracket is first made from the motor and battery size as a reference design; then, the main trigger structure is designed, and the leg structure and electronic control part are designed.

4.1.1. Stents

The holder connects the various parts. The top end of the bracket is used to fix the end of the rubber ring; the upper part is used to place a trigger device composed of a cam, a rod, a magnetic encoder, and a small magnetic plate sensed by the magnetic encoder is placed in the middle of the cross. Here is a physical image of the stand:

4.1.2. Lever

The tie rod comprises two connected triangles. The triangle's three vertices are equipped with bearings in the vertex in the lower right corner, which changes the sliding friction between the cam and the tie rod to rolling friction to reduce resistance. There is a partition between the vertices in the upper left corner. The line starts from here, passes through the bracket, and finally connects between the rear legs. The apex in the lower left corner secures the entire lever to the stand.

4.1.3. Function Board

In order to reduce the use of some DuPont cables to save space, a functioning board was used to place the core controller, motor driver, and step-down module together, and the tin was used for soldering the circuit on the back. As shown in Figure 2, the upper left corner is the core controller, and the upper right side is the motor driver and step-down module, respectively.

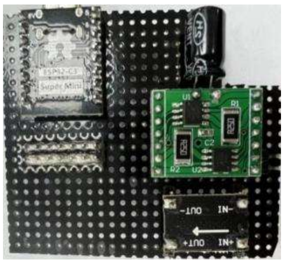

Figure 2. Physical map of the function board

4.1.4. Cams

The cam (shown in Figure 3) is designed using the Archimedean spiral equation and is the area swept by a spiral with an angle between 0° and 540°. When the cam rotates clockwise, the lever remains tangent to its vertex. When the cam turns to the highest point, the tie rod will have a large drop, driving the rope and further releasing the stored spring elastic potential energy. The cam mainly acts as a trigger mechanism in the overall structure.

In order to increase torque further, a pair of reduction gears were added to the motor. In order to obtain a higher transmission ratio and take into account the size of the Robot, a smaller module 1 was selected. The large gear indexing circle is 24mm, the pinion is 7mm, and the pinion is the active gear; the two gears mounted on the transmission shaft of the deceleration motor mesh with each other, and their deceleration ratio is 7:24.

Figure 3. Actual image of the cam (the transparent part is the cam, the pink part is the gear)

4.1.5. Hind leg

The back leg (as shown in Figure 4) is divided into three small parts. The first part is the thigh. The thigh on one side consists of two long acrylic panels to make the thigh stronger. Secure an 11.1V battery (blue part in Figure 4) and a long screw to wrap the cable in the middle of the thigh on both sides and pull the entire rear leg through this wire to move. The second part is the calf. The main function is to adjust the jumping position of this locust bionic robot. The third part is the rear foot (Figure 5). Silicone balls are used on the back foot to increase the coefficient of friction.

Figure 4. Physical map of the overall structure of the rear leg

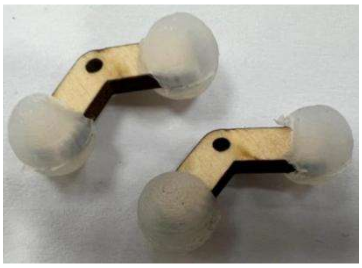

Figure 5. Physical map of the rear foot

4.1.6. Front Leg

The front leg part (shown in Figure 6) consists of two curved front legs and a gear, which mainly supports and adjusts the jumping angle of the Locust robot after landing.

Figure 6. Physical map of the rear foot

Figure 6 Physical view of the front leg (the pink part is the front leg, the transparent part is the gear)

4.2. Second Edition

The jump height and horizontal distance of the first version of the Robot could have been better, so many improvements were made, resulting in the second version.

4.3. Third Edition

Improvements have also been made based on the second version of the Robot. In particular, the leg structure has been added, and newly designed feet have been added to increase friction, thereby further improving the distance and height and adding an automatic correction function to arrive at the third version of the Robot. The following is an introduction to some of the new components and functions:

4.4. Fourth Edition

Locust robots often roll over and fall when the center of gravity is unstable. To solve this problem, an auxiliary automatic correction structure has now been designed. This structure mainly consists of a steering wheel and a cross-standing foot bar structure. When the Robot falls and overturns, the MPU6050 gyroscope installed inside it will read the angle data and print it out through a serial port to monitor the device's attitude in real time. When the angle read by the gyroscope reaches the set mark position, the foot bar will be connected to the steering wheel to swing to correct it automatically.

4.5. Electronic Components

ESP32C3 core controller, A4950 motor driver, DC-DC 3A step-down module, CYS-S0307 analog servo, AS5600 magnetic encoder, N20 DC deceleration motor.

5. Program Design

5.1. Program Overview

This project program was designed and completed by the ESP32C3 MCU, which uses C++ as the programming language. The code written for this Robot enables the locust bionic robot's steering wheel angle and pin level state to be controlled through sliders and buttons and communicated with the Blinker platform.

6. Experiment

In order to verify the accuracy of the mathematical model and discuss the factors affecting the jumping height of the locust robot, an experiment was first designed and carried out to verify the influence of various factors on the Robot's jump using a control variable method. I designed several control groups with different parameters in the experiment, controlled changes in different foreleg height, takeoff height, and center of gravity position parameters, and conducted experiments. I used a tracker to collect and analyze data. The following experimental data and conclusions were obtained.

6.1. Front Leg Gasket Thickness Test (Using the First Version of the Robot)

Test the jump height and distance of the Locust robot by adjusting the thickness of the foreleg pads. Collect experimental data and draw a line chart.

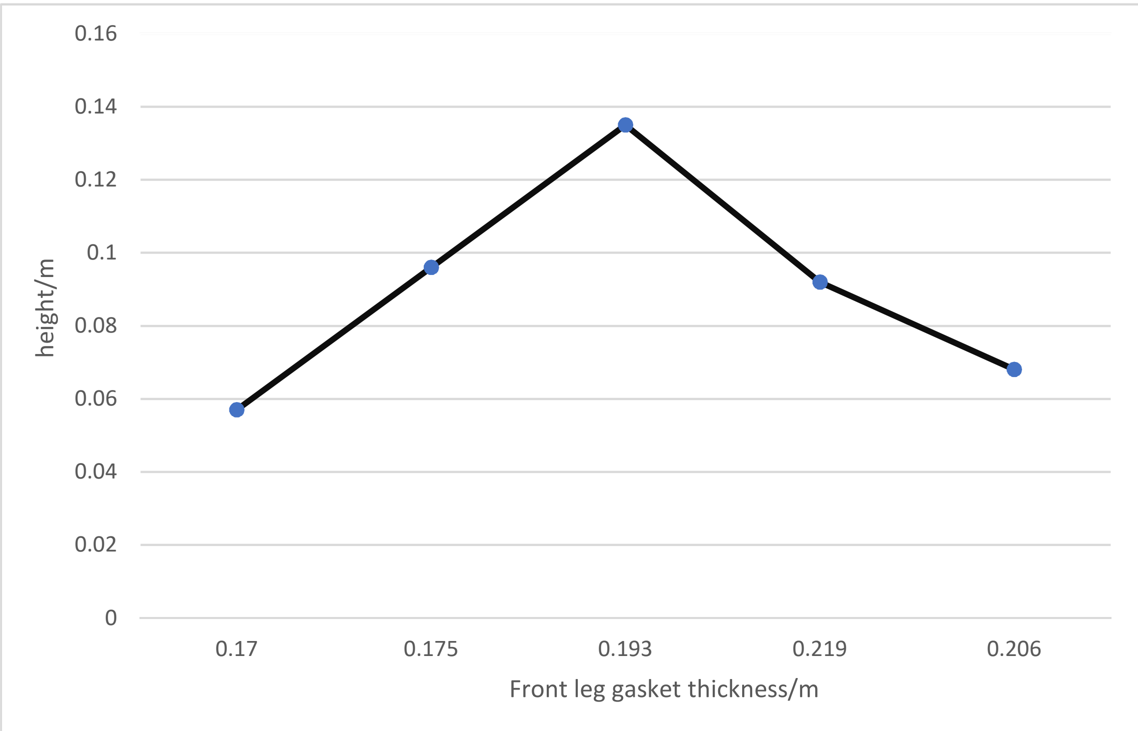

Figure 7. Front leg gasket thickness test line chart

Experimental results showed that when the height of the foreleg gasket was about 19 cm, the locust robot could jump the highest. When the height of the front legs is low, the starting angle is too small, and the Robot mainly jumps forward. When the height of the front leg is too high, the angle between the thigh and calf increases after takeoff, and the total length becomes longer. It will collide with the front leg gasket and lose energy.

Table 1. Front leg gasket thickness test (first version robot)

	Front leg gasket thickness/m	height/m
The first time	0.170	0.057
The second time	0.175	0.096
The third time	0.193	0.135
The Fourth time	0.219	0.092
The fifth time	0.206	0.068

6.2. Starting angle experiment (3rd edition robot)

In order to verify the final formula of the mathematical model in the second part of the mathematical model, the starting angle of the third version of the Locust robot was adjusted in this section. Then, the jump height distance was measured. The results obtained are shown in Table 2.

Table 2. Starting Angle Test Results Table (Third Edition Robot)

	Start angle/degree	distance/m	height/m
The first time	43.7	0.439	0.361
The second time	45.2	0.417	0.331
The third time	52.2	0.403	0.338
The Fourth time	57.6	0.449	0.322
The fifth time	60.9	0.227	0.325

Because locusts all have a starting angle of fewer than 90 degrees, that isθ_k, the larger $sin\theta_k$the larger the takeoff angle, the smaller v_k(initial speed), and the distance of the final movement should be smaller, according to the model, when controlling the rest of the variables. A line chart is drawn from experimental data (Figure 8):

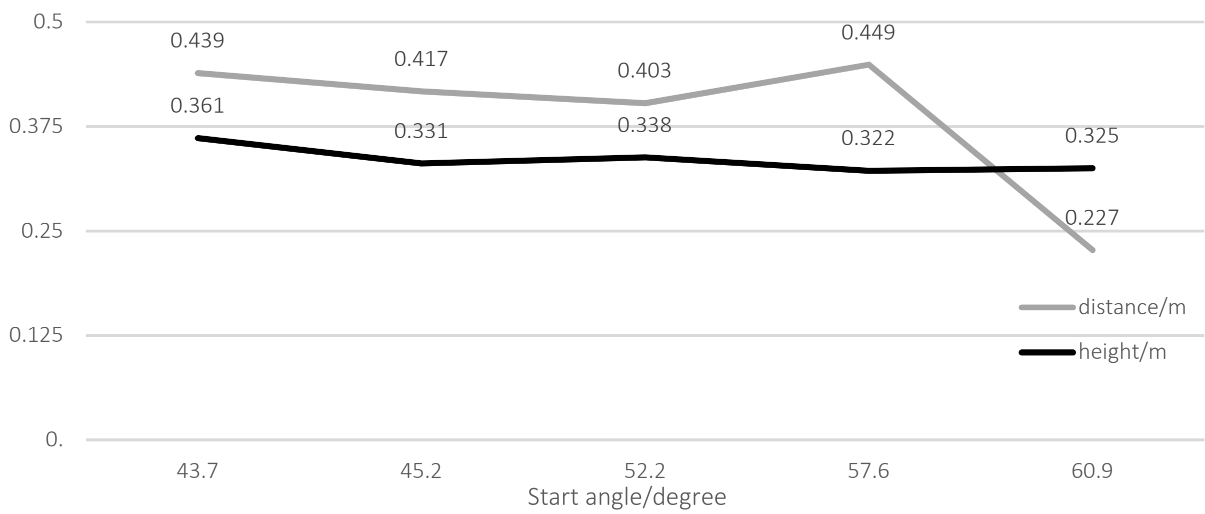

Figure 8. Results of the third edition of the robot experiment

As can be seen, the experimental results are consistent with the results of the theoretical model.

6.3. Center of Gravity Position Experiment (4th Edition Robot)

During the center of gravity position test, adjust the center of gravity by attaching a 15g weight to a certain position from the bottom of the Robot's rear leg.

Table 3. Center of gravity position test results table (4th edition robot)

	Distance between weight and bottom/m	height/m	distance/m
The first time	0.053	0.437	0.638
The second time	0.072	0.500	0.763
The third time	0.104	0.522	0.831
The Fourth time	0.000	0.439	0.563

The line chart below can be drawn from the data in the table above. It is not difficult to conclude that when the center of gravity is high, the Robot will achieve a higher bounce height and distance. According to data, this phenomenon occurs when an object jumps, and its horizontal distance is determined by initial speed, launch angle, and air resistance. Assuming that the initial speed and launch angle are the same, a high center of gravity usually results in a longer horizontal distance because it has a greater vertical velocity component at the moment of the jump.

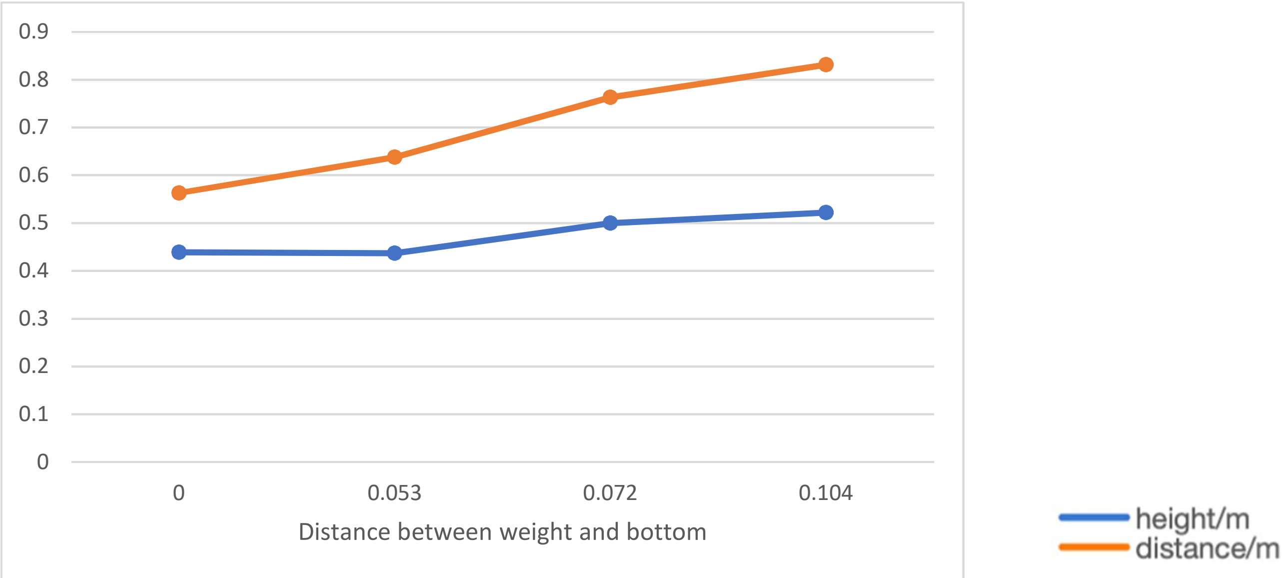

Figure 9. Results of the third edition of the robot experiment

First, let us say an object jumps from the ground, and its center of gravity is lower. Since it is close to the ground during takeoff, it is more affected by gravity, which causes it to fall faster. In this case, the object's flight time is relatively short, so its horizontal displacement is also short.

7. Summary and Outlook

Through intensive experimental verification and research about locusts' jumping ability and stability, this study built a series of jump models and dynamic equations and validated them through experiments. The performed trials made it clear that the initial angle and the point at which the center of gravity was changed were crucial in determining the locust robot's jumping ability.

Automation in the future can also lead to perfection in locust robot design and control algorithm with the aim of improving the jumping movement and balancing dynamics. These goals can be achieved by introducing greater complexity to the mechanical structure and material properties, which are supposed to resemble the locust musculature and elasticity for a more realistic and efficient jumping performance. Moreover, the performance of locust robots with regard to adaptability under different terrain and

References

[1] ZiQiang Zhang, Qi Yang, Shun Gui, Bin Chang, Jing Zhao, HaiSheng Yang, and DianSheng Chen. Mechanism Design for Locust-inspired Robot with One-DOF Leg Based on Jumping Stability [J]. Mechanism and Machine Theory, 2019, 133:584-605.

[2] V. Zaitsev, A. Beck, O. Gvirsman, U. Ben-Hanan, A. Weiss, A. Ayali, and G. Kosa. Miniature Jumping Robot Inspired by Locust [C]. The 5th Israeli Conference on Robotics, 2016.

[3] Yaolei Shen, Wenjie Ge, Xiaojuan Mo, and Zhenghang Hou. Design of a locust-inspired miniature jumping robot [C]. IEEE International Conference on Robotics and Biomimetics (ROBIO), 2018, 2322-2327.

[4] Mo Xiaojuan, Ge Wenjie, Ren Yifei, Zhao Donglai, Wei Dunwen. Locust-like eight-pole jumping robot design based on takeoff stability [J]. Journal of Mechanical Engineering, 2023, 59 (5): 41-52.

[5] Diansheng Chen. Prototype Design and Experimental Study on Locust Air-Posture Righting [J]. Journal of Bionic Engineering 11 (2014): 459-468

[6] Valentin Zaitsev, Omer Gvirsman, Uri Ben Hanan, Avi Weiss, Amir Ayali, and Gabor Kosa. A locust-inspired miniature jumping robot [J]. Bioinspiration & Biomimetics, 2015, 10 (6): 066012.

[7] Jun Zhong, Chun Zhao, and Hui Su. A Novel Locust-inspired Jumping Robot Driven by Pneumatic Muscle Actuators [J]. Advances in Engineering Research, 2018, 170:1732-1735.

[8] Giuliano Punzo and Euan W McGookin. Engineering the Localities: Hind Leg Modelling towards the Design of A Bio-inspired Space Hopper. Proceedings of the Institution of Mechanical Engineers, Part K: Journal of Multi-body Dynamics, 2016, 230(4):455-468.

[9] Songsong Ma, Bing Li, and Yao Li. The Steering Jump Control of a Locust Bio-Robot via Asynchronous Hindleg Kickings Advanced Intelligent Systems, 2022, 4:2200082.